

## Effect of silver ion implantation on antibacterial ability of polyethylene food packing films

Lu, N.; Chen, Z.; Zhang, W.; Yang, G.; Liu, Q.; Böttger, R.; Zhou, S.; Liu, Y.;

Originally published:

February 2021

**Food Packaging and Shelf Life 28(2021), 100650**

DOI: <https://doi.org/10.1016/j.fpsl.2021.100650>

Perma-Link to Publication Repository of HZDR:

<https://www.hzdr.de/publications/Publ-32456>

Release of the secondary publication  
on the basis of the German Copyright Law § 38 Section 4.

CC BY-NC-ND

---

# Effect of silver ion implantation on antibacterial ability of polyethylene food packing films

Naiyan Lu<sup>a</sup>, Zhe Chen<sup>a,\*</sup>, Wei Zhang<sup>a</sup>, Guofeng Yang<sup>a</sup>, Qingrun Liu<sup>e</sup>, Roman Böttger<sup>d</sup>, Shengqiang Zhou<sup>d</sup>, Yu Liu<sup>b,c,d,\*</sup>

<sup>a</sup> State Key Laboratory of Food Science and Technology, Jiangnan University, Wuxi, Jiangsu 214122, China

<sup>b</sup> Microsoft Quantum Materials Lab Copenhagen, Lyngby 2800, Denmark

<sup>c</sup> Center for Quantum Devices, Niels Bohr Institute, University of Copenhagen, Copenhagen 2100, Denmark

<sup>d</sup> Helmholtz-Zentrum Dresden-Rossendorf, Institute of Ion Beam Physics and Materials Research, Dresden 01328, Germany

<sup>e</sup> State Key Laboratory of Food Nutrition and Safety, College of Food Science and Engineering, Tianjin University of Science & Technology, Tianjin 300457, China

**Abstract:** Bacterial adhesion on medical instruments' and food packages' surfaces causes implanted infections, food spoilage and human disease, therefore attracts a lot of attention in the field of medical and food applications. Containing the initial adhesion of bacteria on the surface of the material plays an important role in reducing potential safety hazards. In this work, we investigate the influence of silver ion implantation with different doses on the antibacterial performance of the polyethylene (PE) films. It is found out that silver ion implantation will not color the PE films but can improve their surface hydrophilicity. The silver-implanted PE films show the ability to inhibit bacterial adhesion and have the bactericidal effect, both of which can be improved with increasing silver implantation dose. This method also proves relatively safe, because the silver ions are relatively stable. The results will introduce potential applications for ion implantation in the food packing and food accessible materials.

**Keywords:** polyethylene; ion implantation; surface modification; bacterial adhesion; antibacterial ability; hydrophilicity.

---

\*Corresponding author.

E-mail addresses: [jiz.chen@foxmail.com](mailto:jiz.chen@foxmail.com) (Z. Chen), [yu.liu@nbi.ku.dk](mailto:yu.liu@nbi.ku.dk) (Y. Liu)

---

27 **1. Introduction**

28 Bacterial adhesion is the initial stage of pathogen biofilm formation and the  
29 formation of biofilms is the main cause of food-borne diseases (Erdem et al., 2017).  
30 During the processing of food, the food can be contaminated by microorganisms and  
31 become the source of cross-infection (Trachoo, Frank, & Stern, 2002). Moreover,  
32 microorganisms will be attached to food processing materials, conveying pipes, filter  
33 membranes and heaters to increase work resistance and reduce work efficiency (Miao  
34 et al., 2017), resulting in huge economic losses (Scharff, 2012; Wei, Helm,  
35 Corner-Walker, & Hou, 2006).

36 The biofilm formation process is postulated to have several major stages,  
37 including (I) initial reversible attachment, (II) a transition to irreversible attachment,  
38 (III) biofilm architecture development, (IV) mature biofilm formation, and (V) cell  
39 dispersion (Chao & Zhang, 2011; Fysun, Kern, Wilke, & Langowski, 2019; Renner &  
40 Weibel, 2011). Because mature biofilms have strong resistance to their living  
41 environment, and conventional fungicides cannot remove biofilms effectively (Bridier,  
42 Briandet, Thomas, & Dubois-Brissonnet, 2011; Escribano-Viana et al., 2018; Houari  
43 & Di Martino, 2007; Otter, Yezli, Salkeld, & French, 2013; Sav et al., 2018).  
44 Therefore, it is very important to inhibit bacterial adhesion and to control the biofilm  
45 formation in its early stage (Brecher & Hay, 2005; Lindsay & Von Holy, 2006;  
46 Shorten, Pleasants, & Soboleva, 2006; Zhang, Chao, Shih, Li, & Fang, 2011).

47 Ion implantation has become a hotspot in material modification methods in  
48 recent years (Li et al., 2019; Shiao et al., 2019; Xia et al., 2018; Zheng, Qian, & Liu,  
49 2020). The ions generated by an ion source are shot to the surface of the materials at  
50 high speed. The energetic ions enter the surface, collide with the atoms in the solid,  
51 and finally stop in the materials and are embedded beneath the surface. During this  
52 process, some atoms are displaced, causing changes of the surface composition,  
53 structures, or properties of the materials, and thus serving purposes of modifications  
54 (Hu, Liu, Gan, & Long, 2019; Li et al., 2019). Especially, the ion implantation  
55 technology can adjust hydrophobicity of the surface (Price, Waters, Williams, Lewis,  
56 & Stickler, 2002; Tsuji et al., 2007) and improve the tissue compatibility by changing  
57 the chemical composition of the material surface (Wang et al., 2014), which can  
58 influence the materials' antibacterial adhesion. Hu et al. (Hu, Liu, Gan, & Long, 2019)  
59 have injected Fe<sup>3+</sup> into graphene to improve the stability of the prepared material and  
60 its ability of inhibiting *E. coli*. Price C. et al. (Price, Waters, Williams, Lewis, &  
61 Stickler, 2002) have used argon-plasma bombardment for surface modification, which

---

62 has caused the incorporation of either hydrophilic or hydrophobic functional groups  
63 onto the surface. It turns out that the adhesion of *Candida* has been reduced. Zahran M.  
64 K. et al. (Zahran, Ahmed, & El-Rafie, 2014) have investigated antimicrobial activities  
65 by applying AgNPs–alginate composite on cotton fabric. The treated fabrics show the  
66 excellent antibacterial activity against *P. aeruginosa*, *S. aureus* and *E. coli*.

67 As a broad-spectrum antibacterial agent, silver is one of the most commonly used  
68 antibacterial agents at present (Marchetti et al., 2016; Sahai, Gaval, & Bhat, 2020;  
69 Sanchez-Valdes et al., 2018; Zheng et al., 2016). Tambur P et al. (Tambur, Bhagawan,  
70 Kumari, & Kasa, 2020) have decorated silver nanoparticles on functionalized  
71 multi-walled carbon nanotubes, which has proved to be effective against *Bacillus*  
72 *subtilis*, *S. aureus*, *E. coli*, *P. aeruginosa*. Oses J. et al. (Oses et al., 2014) have found  
73 that silver ions implanted into CrN layers have positive antibacterial effects on *S.*  
74 *aureus* and *E. coli*. However, there are concerns about whether silver can be applied in  
75 the food field efficiently and safely because it is a kind of heavy metal which can  
76 endanger human bodies (Marambio-Jones & Hoek, 2010; Zhang, Wang, & Levanen,  
77 2013). Hadrup, N. et al (Hadrup, Sharma, Loeschner, & Jacobsen, 2020) evaluated  
78 silver to be genotoxic in vitro in mammalian cells. When silver ions are used in food  
79 packing or contact materials, there will be potential risks. Therefore, it is important to  
80 guarantee the antibacterial ability of silver ion fungicides and improve their safety at  
81 the same time. In this study, ion implantation was used to introduce silver ions at  
82 different doses in the food packing material – PE films (Figure 1). The treated films  
83 show the ability of inhibiting bacterial adhesion and bacterial growth on the surface.  
84 The safety of the implanted materials was evaluated with dissolution experiments.

## 85 **2. Materials and methods**

### 86 2.1. Materials

87 *E. coli* BL21, *S. aureus* 6538, and *P. aeruginosa* ATCC 9027 were purchased  
88 from China General Microbiological Culture Collection (CGMCC, Beijing, China).  
89 Luria Bertani (LB) agar and broth, M63 medium and tryptic soy broth (TSB) medium  
90 were purchased from Hepobio Company, Zhengzhou, Henan, China. All other  
91 chemical reagents (AR grade) were purchased from Sinopharm Chemical Reagent Co.,  
92 Ltd. (Shanghai, China) and used as received.

### 93 2.2. Silver ion implantation

94 We used the ion implanter (High Voltage Engineering Europa B.V.,

---

95 Model B8385) at the Ion Beam Center, Helmholtz-Zentrum Dresden-Rossendorf,  
96 Germany. It can provide all kinds of stable ions with the energy from 10 to 500 keV.  
97 The fluence can be from  $5e^{10}$  to  $5e^{16}$   $\text{cm}^{-2}$ . In detail, the Ag ions were produced by a  
98 IHC Bernas ion source. They were electrostatically accelerated to the designed high  
99 voltage. Together with a magnetic analyzer, ions can be selected according to their  
100 atomic mass. To ensure the uniformity, the beam was rastered over the sample. The  
101 PE films with area of  $100 \text{ mm} \times 100 \text{ mm}$  were implanted with different doses of silver  
102 ions. The beam energy was set to 190 keV, the temperature of PE films was kept less  
103 than  $50^\circ\text{C}$ , and the implantation angle was  $7^\circ$ . The injection doses were as follows,  
104 sample 0: none, sample 1:  $5 \times 10^{12} \text{ cm}^{-2}$ , sample 2:  $1 \times 10^{13} \text{ cm}^{-2}$ , sample 3:  $5 \times 10^{13} \text{ cm}^{-2}$ ,  
105 sample 4:  $1 \times 10^{14} \text{ cm}^{-2}$ , sample 5:  $5 \times 10^{14} \text{ cm}^{-2}$ , and sample 6:  $1 \times 10^{15} \text{ cm}^{-2}$ .

### 106 2.3. Contact angle measurement

107 The water contact angles of PE film were measured using a Krüss DSA100 Drop  
108 Analysis System (Krüss GmbH, Hamburg, Germany) at room temperature ( $\sim 20^\circ\text{C}$ ). 1  
109  $\mu\text{L}$  of DI water was added on the film surface. The contact angles were calculated  
110 using the DSA Registered Version software provided with the instrument. And the  
111 final result of water contact angle values was obtained by calculating the average of  
112 values in triplicate at different positions of the PE film after ion implantation.

### 113 2.4. Bacterial strains and bacterial attachment experiments

114 *E. coli* BL21, *S. aureus* 6538, and *P. aeruginosa* ATCC 9027 were inoculated  
115 into LB agar plates, and then transferred into LB broth with agitation at  $37^\circ\text{C}$ , 200  
116 rpm for 12 h. The incubated cells were harvested in log phase, centrifuged (5000 g)  
117 for 15 min at  $4^\circ\text{C}$ , and washed twice with 0.08 M phosphate buffer saline (PBS, pH  
118 7.4). The *E. coli* suspensions were diluted with PBS until the optical density at 600  
119 nm equaled  $0.6 \pm 0.05$  (approximately  $10^8$  CFU/mL), and transferred into M63 medium  
120 with 1% (Friedlander et al., 2013). *S. aureus* and *P. aeruginosa* were added into TSB  
121 medium at the same concentration. PE films were placed at the bottom of a 6-well  
122 tissue culture plate at least in triplicate; M63 medium with *E. coli*, TSB medium with  
123 *S. aureus* or *P. aeruginosa* were poured into the 6-well tissue culture plate to cover the  
124 film. The plates were incubated at  $37^\circ\text{C}$  for 5 h.

### 125 2.5. Determination of resistance to bacterial growth

126 *E. coli* BL21, *S. aureus* 6538, and *P. aeruginosa* ATCC 9027 were inoculated  
127 into LB agar plates, and then transferred into LB broth with agitation at  $37^\circ\text{C}$ , 200

---

128 rpm for 12 h. The incubated cells were harvested in log phase. The three strains were  
129 separately diluted to make the concentration of the bacterial suspension  $10^5$ - $10^6$   
130 CFU/mL.

131 Refer to "Antibacterial products-Test for antimicrobial activity and Effects"  
132 (Japanese Industrial Standard JIS Z2801-2000). Each PE film after the silver ion  
133 implantation was cut into samples with a size of 1 cm×1 cm, washed with 70%  
134 ethanol, dried with nitrogen. 100  $\mu$ L bacterial suspension was added on the surface of  
135 the film, and then it was covered with a sterile film.

136 The bacterial solution was evenly coated on the surface of the film, and the  
137 relative humidity of the incubator was adjusted to be more than 90%. After incubating  
138 in a 37°C incubator for 24 h, the film was taken out and rinsed with sterile  
139 physiological saline. Then, the eluent was inoculated into LB solid medium to  
140 cultivate in a 37°C incubator for 24 h. After cultivating, plate colony count was  
141 performed and recorded as  $A_t$ . Meanwhile, the number of plate colonies in the control  
142 group without silver ion implantation treatment was recorded as  $A_0$ . The calculation  
143 formula of antibacterial rate is as follows:

$$144 \quad \textit{Antibacterial rate (\%)} = (A_0 - A_t) / A_0 \times 100\%$$

## 145 2.6. Silver ion dissolution determination

146 After the silver ion implantation, each PE film was cut into samples with a size  
147 of 1 cm × 1 cm, washed with 70% ethanol and dried with nitrogen. Then we placed  
148 the material into 2 mL ultrapure water to soak it in the condition of 37°C for 24 h. In  
149 the end, the water samples were collected and the content of silver ions was  
150 determined by atomic absorption spectrophotometer.

## 151 2.7. Confocal scanning laser microscopy (CLSM)

152 *E. coli*, *S. aureus* and *P. aeruginosa* grown on PE films were rinsed and fixed  
153 using the method of Friedlander et al. (Friedlander et al., 2013). Cells were  
154 permeabilized with 0.1% Triton X-100 in PBS for 15 min. Samples were then stained  
155 with Fluorescein isothiocyanate (FITC), 10 mg/mL for 30 min, and rinsed with PBS  
156 twice. PE films were placed face-down on a glass-bottomed sample dish (Shengyou  
157 Biotechnology Co., Ltd, Hangzhou, Zhejiang, China) and placed on the stage of the  
158 confocal laser scanning microscope (CLSM 710, Zeiss, Oberkochen, Germany).  
159 CLSM is equipped with an Ar laser at 488 nm. Images were obtained using the 63×oil  
160 immersion lens and processed using Image J software (NIH, Bethesda, MD, USA).

161 Three different fields of view were randomly chosen for analysis of the percentage of  
162 the images that show bacterial adhesion of the films.

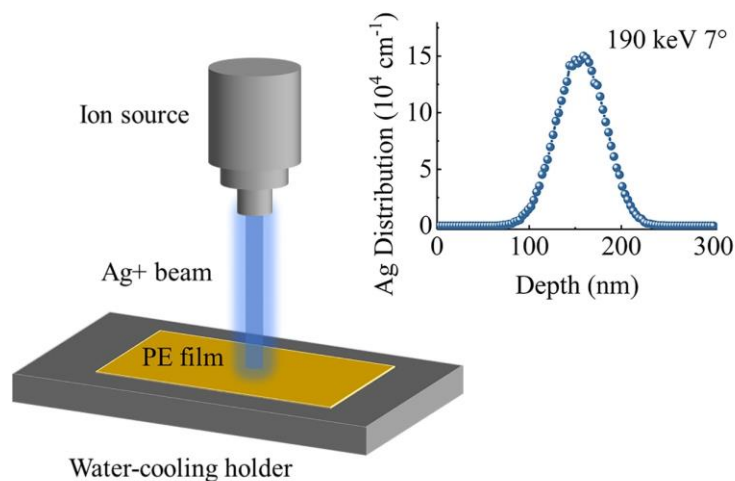
## 163 2.8. Statistical analysis

164 Statistical analysis was conducted using SPSS Statistics 20.0, where  $p < 0.05$  was  
165 used as the standard for significance. Origin 2018 and EXCEL 2016 were used to plot  
166 and analyze the data.

## 167 3. Results and discussion

### 168 3.1. Characterization of surface properties of PE film after silver ion implantation

169 In the condition of 190 keV and an angle of  $7^\circ$ , the stretched PE film was  
170 implanted with silver ions of different doses. According to the ion implantation  
171 simulation with SRIM (Stopping and Range of Ions in Matter), it can be seen that the  
172 silver element is mainly distributed at a depth of 75~250 nm, and the highest dose is  
173 at a depth of 170 nm, as shown in the inset of Figure 1. This result illustrates that the  
174 ion implantation only modifies the surface.

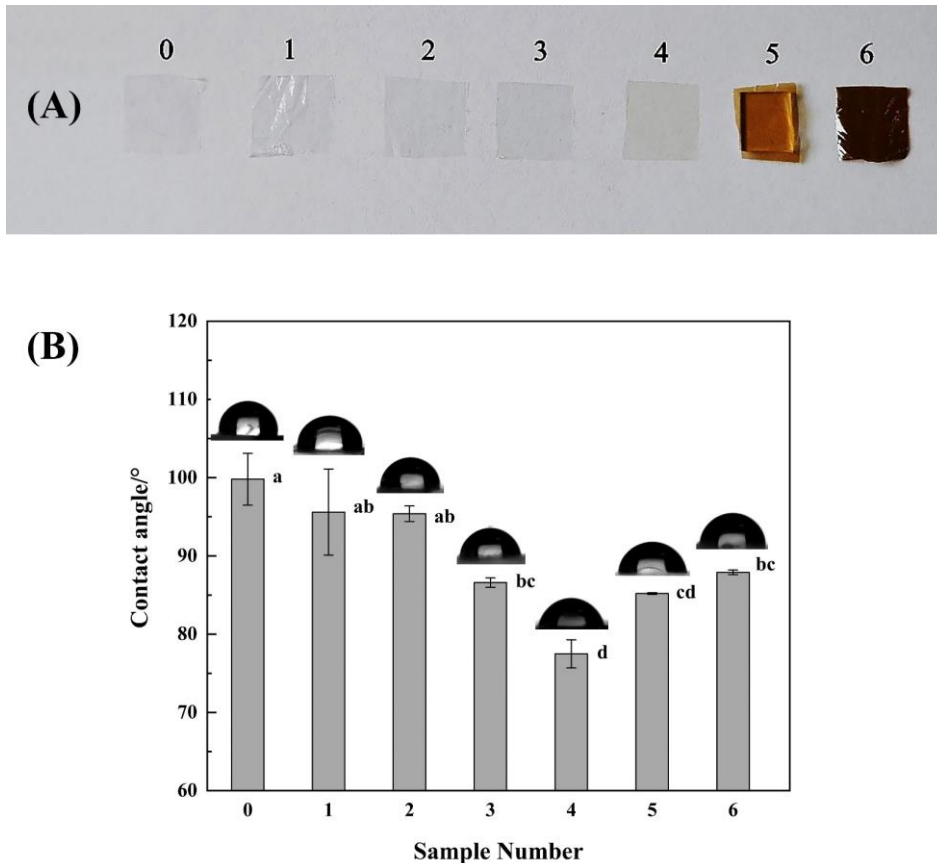


175

176 **Fig. 1.** The schematic of silver ion implantation on a PE film. Inset: Ag depth distribution on PE  
177 films after implantation.

178 The appearance of the stretched film which has been ion-implanted is shown in  
179 Figure 2(A). It can be found out that the color of the material was changed after the  
180 silver ion implantation. Samples 1-3 is similar to the control group (sample 0), which  
181 is still colorless and transparent. Sample 4 shows yellowish and sample 5 appears  
182 brown, but they are still translucent. Sample 6 has almost no transparency, appearing  
183 dark brown. In comparison with the control group, it can be found out that samples 5  
184 and 6 become brittle and the toughness deteriorates largely. This phenomenon

185 indicates that different doses of silver ion implantation have different influence on the  
186 surface of the PE film.



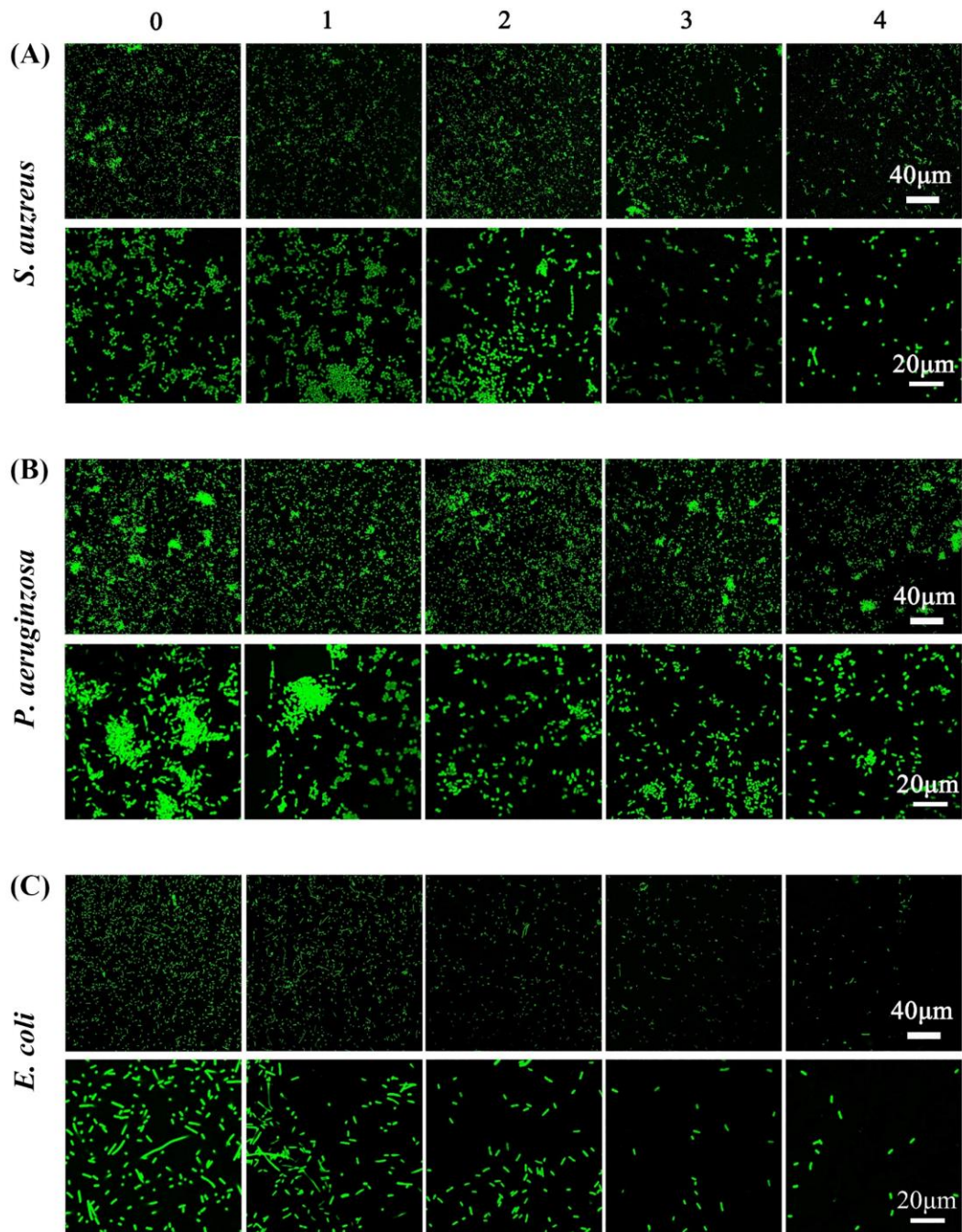
187  
188 **Fig. 2.** The samples(A) and the contact angles(B) of PE films after ion implantation with different  
189 doses. 0: None, 1:  $5 \times 10^{12} \text{ cm}^{-2}$ , 2:  $1 \times 10^{13} \text{ cm}^{-2}$ , 3:  $5 \times 10^{13} \text{ cm}^{-2}$ , 4:  $1 \times 10^{14} \text{ cm}^{-2}$ , 5:  $5 \times 10^{14} \text{ cm}^{-2}$ , 6:  
190  $1 \times 10^{15} \text{ cm}^{-2}$ , where  $P < 0.05$ .

191 The surface contact angle of samples 0 to 6 was measured in Figure 2(B).  
192 Compared with the control group, the contact angle of the PE film after silver ion  
193 implantation (sample 4) decreased by 24 from 100, indicating that silver ion  
194 implantation has improved the surface hydrophilicity of the material. The main reason  
195 is that silver ion implantation increases the surface roughness of the material. At the  
196 same time, the addition of silver ion itself changes the interaction force between water  
197 and the surface of the material. On the other hand, the contact angle increases for  
198 samples 5 and 6, suggesting that the surface roughness decreases. It can be understood  
199 as the excessive implantation doses damaged the internal molecular structure and the  
200 PE films were melted and reconstituted. Therefore, the samples 5 and 6 are not  
201 suitable for food packing materials or food contact materials because of their color

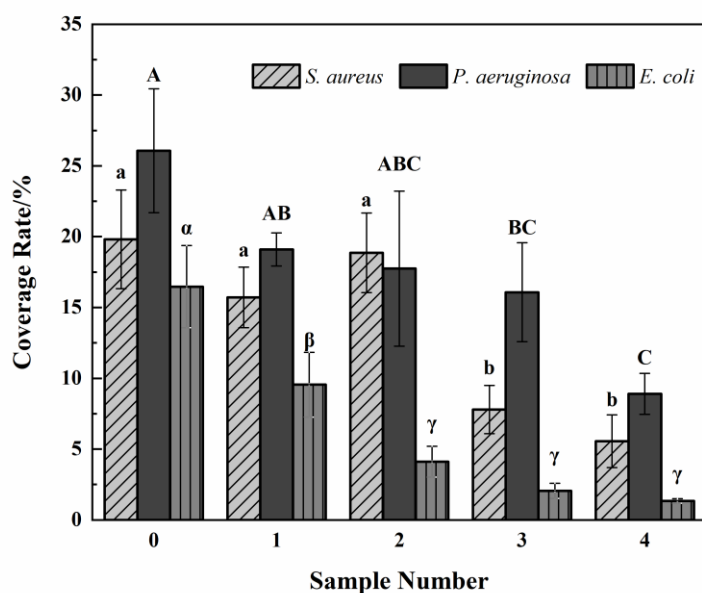


202 and change of structures. Based on these reasons, further measurements are only  
203 performed for samples 0-4.

204 3.2. Antibacterial adhesion of films



205  
206 **Fig. 3.** CLSM images of *S. aureus*(A), *P. aeruginosa*(B) and *E. coli*(C) adhesion on PE films after  
207 ion implantation with different doses. 0: None, 1:  $5 \times 10^{12} \text{ cm}^{-2}$ , 2:  $1 \times 10^{13} \text{ cm}^{-2}$ , 3:  $5 \times 10^{13} \text{ cm}^{-2}$ , 4:  
208  $1 \times 10^{14} \text{ cm}^{-2}$ .



209

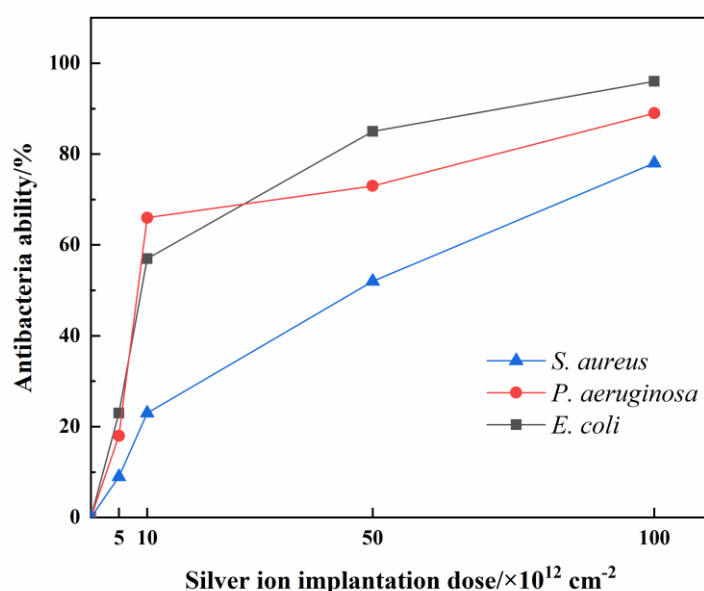
210 **Fig. 4.** The coverage rate of *S. aureus*, *P. aeruginosa* and *E. coli* counted base on the CLSM  
 211 images. Histograms labeled with different letters (a-c, A-C, α-γ) represent significant differences.

212 Strong antibacterial adhesion can effectively hinder the formation of bacterial  
 213 biofilm and slow down bacterial reproduction speed. The bacterial adhesion was  
 214 identified by CLSM technology. The adhesion of *S. aureus*, *P. aeruginosa* and *E. coli*  
 215 on the silver ion-implanted PE film is shown in Figure 3 and 4. For *S. aureus*, the  
 216 adhesion of sample 2 was large, and samples 3 to 4 began to show a certain degree of  
 217 inhibition. Sample 0-2 had a certain amount of bacterial cell agglomeration, which  
 218 also indirectly illustrated that sample 3 and 4 have an inhibitory effect on the  
 219 subsequent biofilm formation of *S. aureus*. For *P. aeruginosa*, samples 3 and 4 had  
 220 inhibitory effects, and there were more single cell adhesion and no obvious bacterial  
 221 aggregation, which indicated that the samples had a certain inhibitory effect on the  
 222 subsequent biofilm formation. For *E. coli*, sample 2-4 all showed a good inhibitory  
 223 effect. Comparing the adhesion of the three strains on the silver ion-implanted  
 224 samples, it can be found out that, for different bacteria, the silver ion dose required to  
 225 inhibit their adhesion is different. Among the three strains, the *E. coli* requires the  
 226 lowest dose of silver ions, which is related to its poor adhesion ability (Lu et al., 2016);  
 227 doses required against *S. aureus* and *P. aeruginosa* are similar.

228 The surface modification of PE film by silver ion implantation improves the  
 229 ability of PE films to inhibit bacterial adhesion. According to the contact angle results,  
 230 higher doses of silver ion implantation make a PE film more hydrophilic. And the

231 hydrophilic samples should have weak ability to inhibit bacterial adhesion (Lu et al.,  
232 2016). Therefore, the effect of silver ions on bacterial adhesion is greater than that of  
233 hydrophobicity improvement brought by ion implantation.

### 234 3.3. Antibacterial ability of the film



235

236

**Fig. 5.** Antibacterial ability of Ag ion-implanted PE films.

237 To investigate the antibacterial activity after the silver ions are implanted into the  
238 PE films, the quantitative experiments were conducted by the film adhesion method.  
239 As shown in Figure 5, after silver ion implantation, similar to the trend of the bacterial  
240 adhesion results, the antibacterial activity of sample 1 is low. When the silver ion dose  
241 increases, the antibacterial activity of the sample gradually increases. Different  
242 bacteria have different tolerances to silver ions. At a dose of  $1 \times 10^{13} \text{ cm}^{-2}$ , more than  
243 half of *P. aeruginosa* and *E. coli* can be killed. In contrast, the same activity can be  
244 achieved at the dose of  $5 \times 10^{13} \text{ cm}^{-2}$  for *S. aureus*. The activity difference comes from  
245 the different composition and structure of the cell walls of the bacteria. The  
246 peptidoglycan layer of the cell wall of gram-positive bacteria is thick and dense, with  
247 phosphorus acid embedded, less or no lipid, lipopolysaccharide, lipoprotein.  
248 Correspondingly, the cell wall of Gram-negative bacteria is thin and loose, and the  
249 outer membrane is composed by phospholipids, lipopolysaccharides, and proteins  
250 (Silhavy, Kahne, & Walker, 2010).

251 So far, Anh, D. H. et al. (Anh, Dumri, Anh, Punyodom, & Rachtanapun, 2016)  
252 have found that the PE/AgNP nanocomposites restricted common pathogenic bacteria

253 (*E. coli*, *Bacillus subtilis*, *Salmonella typhimurium*) in their early developmental stage.  
 254 Aalaie, J. et al. (Aalaie, Mirali, Motamedi, & Khanli, 2011) have found that PE  
 255 films with as little as 1 wt% nanosilver provided absolute antibacterial performance,  
 256 while generally maintaining the mechanical properties. Marchetti, F. et al.  
 257 (Marchetti et al., 2015) have embedded new silver (I) acylpyrazolonato derivatives  
 258 with mononuclear, polynuclear or ionic properties in a PE matrix and found that most  
 259 of the composite materials have better antibacterial effects. The data in this study  
 260 further shows capability of the relevant materials to break the bacterial cell membrane.  
 261 Brito, S. D. et al (Brilo, Bresolin, Sivieri, & Ferreira, 2020) discovered that the  
 262 packages incorporating silver nanoparticles inhibited the growth and reproduction of  
 263 bacterial cells during the early stages. This is the same view as our study.

#### 264 3.4. Determination of material safety

265 After immersing the samples in 2 mL ultrapure water for 24 h, the concentrations of  
 266 silver ions in the solution were determined by atomic absorption spectroscopy. As  
 267 shown in Table 1, the silver ion concentrations were all below the detection limit of  
 268 the instrument, less than 0.01 mg/L. The silver ions after implantation are relatively  
 269 stable on the surface of the material. This technique does not only guarantee the  
 270 antibacterial activity of silver ions, but also greatly improves its safety. However,  
 271 according to Commission Regulation (EU) No 10/2011 of 14 January 2011 on plastic  
 272 materials and articles intended to come into contact with food, more research should  
 273 be done before the material is applied directly to food and other fields.

274 **Table 1** Dissolution of silver ions from different labels in water.

Label	Implantation dose of silver ions /cm <sup>-2</sup>	Dissolution
0	0	Not detected
1	5×10 <sup>12</sup>	Not detected
2	1×10 <sup>13</sup>	Not detected
3	5×10 <sup>13</sup>	Not detected
4	1×10 <sup>14</sup>	Not detected
5	5×10 <sup>14</sup>	Not detected

#### 275 4. Conclusions

276 We have explored the possibility of the Ag-implanted PE films as antibacterial  
 277 food packing or food contact materials. When a dose is smaller than 1×10<sup>14</sup> cm<sup>-2</sup>,  
 278 silver ion implantation will not color the PE films but can improve their surface

---

279 hydrophilicity. Meanwhile, the PE films show the ability to inhibit bacterial adhesion  
280 and have the bactericidal effect, both of which can be improved at higher doses. This  
281 method is relatively safe, because the silver ions are stable and their dissolution  
282 concentrations are all less than 0.01 mg/L. The results present the potential of ion  
283 implantation in the food packing or food contact materials.

#### 284 **Acknowledgements**

285 This research was supported by the National Natural Science Foundation of  
286 China (31871865, 31401589), the Fundamental Research Funds for the Central  
287 Universities (JUSRP21925), the Science and Technology Development Foundation of  
288 Wuxi (N20191002). The authors gratefully acknowledge the support by the HZDR's  
289 Ion Beam Center (IBC).

---

290 References

- 291 Aalaie, J., Mirali, M., Motamedi, P. & Khanli, H. H. (2011). On the Effect of Nanosilver Reinforcement  
292 on the Mechanical, Physical, and Antimicrobial Properties of Polyethylene Blown Films. *Journal of*  
293 *Macromolecular Science Part B-Physics*, 50(10), 1873-1881. [10.1080/00222348.2011.553174](https://doi.org/10.1080/00222348.2011.553174)
- 294 Anh, D. H., Dumri, K., Anh, N. T., Punyodom, W. & Rachtanapun, P. (2016). Facile fabrication of  
295 polyethylene/silver nanoparticle nanocomposites with silver nanoparticles traps and holds early  
296 antibacterial effect. *Journal of Applied Polymer Science*, 133(17), Article 43331.  
297 <https://doi.org/10.1002/app.43331>
- 298 Brecher, M. E. & Hay, S. N. (2005). Bacterial contamination of blood components. *Clinical*  
299 *Microbiology Reviews*, 18(1), 195-204. <https://doi.org/10.1128/Cmr.18.1.195-204.2005>
- 300 Bridier, A., Briandet, R., Thomas, V. & Dubois-Brissonnet, F. (2011). Resistance of bacterial biofilms  
301 to disinfectants: a review. *Biofouling*, 27(9), 1017-1032.  
302 <https://doi.org/10.1080/08927014.2011.626899>
- 303 Brito, S. D., Bresolin, J. D., Sivieri, K. & Ferreira, M. D. (2020). Low-density polyethylene films  
304 incorporated with silver nanoparticles to promote antimicrobial efficiency in food packaging. *Food*  
305 *Science and Technology International*, 26(4), 353-366. Artn 1082013219894202  
306 [10.1177/1082013219894202](https://doi.org/10.1177/1082013219894202)
- 307 Chao, Y. Q. & Zhang, T. (2011). Probing Roles of Lipopolysaccharide, Type 1 Fimbria, and Colanic  
308 Acid in the Attachment of *Escherichia coli* Strains on Inert Surfaces. *Langmuir*, 27(18),  
309 11545-11553. <https://doi.org/10.1021/la202534p>
- 310 Erdem, E., Yagmur, M., Boral, H., Ilkit, M., Ersoz, R. & Seyedmousavi, S. (2017). *Aspergillus flavus*  
311 Keratitis: Experience of a Tertiary Eye Clinic in Turkey. *Mycopathologia*, 182(3-4), 379-385.  
312 <https://doi.org/10.1007/s11046-016-0089-1>
- 313 Escribano-Viana, R., Lopez-Alfaro, I., Lopez, R., Santamaria, P., Gutierrez, A. R. &  
314 Gonzalez-Arenzana, L. (2018). Impact of Chemical and Biological Fungicides Applied to  
315 Grapevine on Grape Biofilm, Must, and Wine Microbial Diversity. *Frontiers in Microbiology*, 9,  
316 Article 00059. <https://doi.org/10.3389/fmicb.2018.00059>
- 317 Friedlander, R. S., Vlamakis, H., Kim, P., Khan, M., Kolter, R. & Aizenberg, J. (2013). Bacterial  
318 flagella explore microscale hummocks and hollows to increase adhesion. *Proceedings of the*  
319 *National Academy of Sciences of the United States of America*, 110(14), 5624-5629.  
320 <https://doi.org/10.1073/pnas.1219662110>
- 321 Fysun, O., Kern, H., Wilke, B. & Langowski, H. C. (2019). Evaluation of factors influencing dairy  
322 biofilm formation in filling hoses of food-processing equipment. *Food and Bioprocess Processing*,  
323 113, 39-48. <https://doi.org/10.1016/j.fbp.2018.10.009>
- 324 Hadrup, N., Sharma, A. K., Loeschner, K. & Jacobsen, N. R. (2020). Pulmonary toxicity of silver  
325 vapours, nanoparticles and fine dusts: A review. *Regulatory Toxicology and Pharmacology*, 115,  
326 ARTN 104690  
327 [10.1016/j.yrtph.2020.104690](https://doi.org/10.1016/j.yrtph.2020.104690)
- 328 Houari, A. & Di Martino, P. (2007). Effect of chlorhexidine and benzalkonium chloride on bacterial  
329 biofilm formation. *Letters in Applied Microbiology*, 45(6), 652-656.  
330 <https://doi.org/10.1111/j.1472-765X.2007.02249.x>
- 331 Hu, J. H., Liu, J., Gan, L. H. & Long, M. N. (2019). Surface-Modified Graphene Oxide-Based Cotton  
332 Fabric by Ion Implantation for Enhancing Antibacterial Activity. *Acs Sustainable Chemistry &*  
333 *Engineering*, 7(8), 7686-7692. <https://doi.org/10.1021/acssuschemeng.8b06361>

---

334 Li, J., Hou, X. G., Sun, T. T., Han, J., Liu, H. L. & Li, D. J. (2019). Hydrophilic, antibacterial and  
335 photocatalytic properties of TiO<sub>2</sub> composite films modified by the methods of N<sup>+</sup> ion implantation  
336 and doping of CNTs. *Surface & Coatings Technology*, 365, 123-128.  
337 <https://doi.org/10.1016/j.surfcoat.2018.07.063>

338 Lindsay, D. & Von Holy, A. (2006). Bacterial biofilms within the clinical setting: what healthcare  
339 professionals should know. *Journal of Hospital Infection*, 64(4), 313-325.  
340 <https://doi.org/10.1016/j.jhin.2006.06.028>

341 Lu, N. Y., Zhang, W., Weng, Y. Y., Chen, X. X., Cheng, Y. & Zhou, P. (2016). Fabrication of PDMS  
342 surfaces with micro patterns and the effect of pattern sizes on bacteria adhesion. *Food Control*, 68,  
343 344-351. <https://doi.org/10.1016/j.foodcont.2016.04.014>

344 Marambio-Jones, C. & Hoek, E. M. V. (2010). A review of the antibacterial effects of silver  
345 nanomaterials and potential implications for human health and the environment. *Journal of*  
346 *Nanoparticle Research*, 12(5), 1531-1551. <https://doi.org/10.1007/s11051-010-9900-y>

347 Marchetti, F., Palmucci, J., Pettinari, C., Pettinari, R., Condello, F., Ferraro, S., Marangoni, M., Crispini,  
348 A., Scuri, S., Grappasonni, I., Cocchioni, M., Nabissi, M., Chierotti, M. R. & Gobetto, R. (2015).  
349 Novel Composite Plastics Containing Silver(I) Acylpyrazolonato Additives Display Potent  
350 Antimicrobial Activity by Contact. *Chemistry-a European Journal*, 21(2), 836-850.  
351 <https://doi.org/10.1002/chem.201404812>

352 Marchetti, F., Palmucci, J., Pettinari, C., Pettinari, R., Marangoni, M., Ferraro, S., Giovannetti, R.,  
353 Scuri, S., Grappasonni, I., Cocchioni, M., Hodar, F. J. M. & Gunnella, R. (2016). Preparation of  
354 Polyethylene Composites Containing Silver(I) Acylpyrazolonato Additives and SAR Investigation  
355 of their Antibacterial Activity. *Acs Applied Materials & Interfaces*, 8(43), 29676-29687.  
356 10.1021/acsami.6b09742

357 Miao, J., Liang, Y. R., Chen, L. Q., Wang, W. X., Wang, J. W., Li, B., Li, L., Chen, D. Q. & Xu, Z. B.  
358 (2017). Formation and development of Staphylococcus biofilm: With focus on food safety. *Journal*  
359 *of Food Safety*, 37(4), Article e12358. <https://doi.org/10.1111/jfs.12358>

360 Oses, J., Palacio, J. F., Kulkarni, S., Medrano, A., Garcia, J. A. & Rodriguez, R. (2014). Antibacterial  
361 PVD coatings doped with silver by ion implantation. *Applied Surface Science*, 310, 56-61.  
362 <https://doi.org/10.1016/j.apsusc.2014.04.043>

363 Otter, J. A., Yezli, S., Salkeld, J. a. G. & French, G. L. (2013). Evidence that contaminated surfaces  
364 contribute to the transmission of hospital pathogens and an overview of strategies to address  
365 contaminated surfaces in hospital settings. *American Journal of Infection Control*, 41(5), S6-S11.  
366 <https://doi.org/10.1016/j.ajic.2012.12.004>

367 Price, C., Waters, M. G. J., Williams, D. W., Lewis, M. a. O. & Stickler, D. (2002). Surface  
368 modification of an experimental silicone rubber aimed at reducing initial candidal adhesion. *Journal*  
369 *of Biomedical Materials Research*, 63(2), 122-128. <https://doi.org/10.1002/jbm.10094>

370 Renner, L. D. & Weibel, D. B. (2011). Physicochemical regulation of biofilm formation. *Mrs Bulletin*,  
371 36(5), 347-355. <https://doi.org/10.1557/mrs.2011.65>

372 Sahai, R. S. N., Gaval, V. R. & Bhat, B. (2020). Preparation of low-density polyethylene-silver ion  
373 antimicrobial film with and without ethylene-vinyl acetate. *Polymers & Polymer Composites*,  
374 28(8-9), 554-561. 10.1177/0967391119892473

375 Sanchez-Valdes, S., Munoz-Jimenez, L., Ramos-Devalle, L. F., Sanchez-Martinez, Z. V.,  
376 Flores-Gallardo, S., Ramirez-Vargas, R. R., Ramirez-Vargas, E., Castaneda-Flores, M.,  
377 Betancourt-Galindo, R., Martinez-Colunga, J. G., Mondragon-Chaparro, M. & Sanchez-Lopez, S.

---

378 (2018). Antibacterial silver nanoparticle coating on oxo-biodegradable polyethylene film surface  
379 using modified polyethylene and corona discharge. *Polymer Bulletin*, 75(9), 3987-4002.  
380 [10.1007/s00289-017-2247-0](https://doi.org/10.1007/s00289-017-2247-0)

381 Sav, H., Rafati, H., Oz, Y., Dalyan-Cilo, B., Ener, B., Mohammadi, F., Ilkit, M., Van Diepeningen, A. D.  
382 & Seyedmousavi, S. (2018). Biofilm Formation and Resistance to Fungicides in Clinically Relevant  
383 Members of the Fungal Genus *Fusarium*. *Journal of Fungi*, 4(1), 16.  
384 <https://doi.org/10.3390/jof4010016>

385 Scharff, R. L. (2012). Economic Burden from Health Losses Due to Foodborne Illness in the United  
386 States. *Journal of Food Protection*, 75(1), 123-131. <https://doi.org/10.4315/0362-028x.Jfp-11-058>

387 Shiau, D. K., Yang, C. H., Sun, Y. S., Wu, M. F., Pan, H. B. & Huang, H. H. (2019). Enhancing the  
388 blood response and antibacterial adhesion of titanium surface through oxygen plasma immersion  
389 ion implantation treatment. *Surface & Coatings Technology*, 365, 173-178.  
390 <https://doi.org/10.1016/j.surfcoat.2018.05.029>

391 Shorten, P. R., Pleasants, A. B. & Soboleva, T. K. (2006). Estimation of microbial growth using  
392 population measurements subject to a detection limit. *International Journal of Food Microbiology*,  
393 108(3), 369-375. <https://doi.org/10.1016/j.ijfoodmicro.2005.11.024>

394 Silhavy, T. J., Kahne, D. & Walker, S. (2010). The Bacterial Cell Envelope. *Cold Spring Harbor*  
395 *Perspectives in Biology*, 2(5), a000414. <https://doi.org/10.1101/cshperspect.a000414>

396 Tambur, P., Bhagawan, D., Kumari, B. S. & Kasa, R. R. (2020). A facile synthesis of implantation of  
397 silver nanoparticles on oxygen-functionalized multi-walled carbon nanotubes: structural and  
398 antibacterial activity. *Sn Applied Sciences*, 2(5), 981. <https://doi.org/10.1007/s42452-020-2797-x>

399 Trachoo, N., Frank, J. F. & Stern, N. J. (2002). Survival of *Campylobacter jejuni* in biofilms isolated  
400 from chicken houses. *Journal of Food Protection*, 65(7), 1110-1116.  
401 <https://doi.org/10.4315/0362-028x-65.7.1110>

402 Tsuji, H., Sommani, P., Kitamura, T., Hattori, M., Sato, H., Gotoh, Y. & Ishikawa, J. (2007). Nerve-cell  
403 attachment properties of polystyrene and silicone rubber modified by carbon negative-ion  
404 implantation. *Surface & Coatings Technology*, 201(19-20), 8123-8126.  
405 <https://doi.org/10.1016/j.surfcoat.2006.01.074>

406 Wang, S. L., Shi, X. H., Yang, Z., Zhang, Y. M., Shen, L. R., Lei, Z. Y., Zhang, Z. Q., Cao, C. & Fan, D.  
407 L. (2014). Osteopontin (OPN) Is an Important Protein to Mediate Improvements in the  
408 Biocompatibility of C Ion-Implanted Silicone Rubber. *Plos One*, 9(6), Article e98320.  
409 <https://doi.org/10.1371/journal.pone.0098320>

410 Wei, J., Helm, G. S., Corner-Walker, N. & Hou, X. L. (2006). Characterization of a non-fouling  
411 ultrafiltration membrane. *Desalination*, 192(1-3), 252-261.  
412 <https://doi.org/10.1016/j.desal.2005.06.049>

413 Xia, C., Cai, D. S., Tan, J., Li, K. Q., Qiao, Y. Q. & Liu, X. Y. (2018). Synergistic Effects of N/Cu Dual  
414 Ions Implantation on Stimulating Antibacterial Ability and Angiogenic Activity of Titanium. *Acs*  
415 *Biomaterials Science & Engineering*, 4(9), 3185-3193.  
416 <https://doi.org/10.1021/acsbiomaterials.8b00501>

417 Zahran, M. K., Ahmed, H. B. & El-Rafie, M. H. (2014). Surface modification of cotton fabrics for  
418 antibacterial application by coating with AgNPs-alginate composite. *Carbohydrate Polymers*, 108,  
419 145-152. <https://doi.org/10.1016/j.carbpol.2014.03.005>



- 
- 420 Zhang, T., Chao, Y. Q., Shih, K. M., Li, X. Y. & Fang, H. H. P. (2011). Quantification of the lateral  
421 detachment force for bacterial cells using atomic force microscope and centrifugation.  
422 Ultramicroscopy, 111(2), 131-139. <https://doi.org/10.1016/j.ultramic.2010.10.005>
- 423 Zhang, X. X., Wang, L. & Levanen, E. (2013). Superhydrophobic surfaces for the reduction of bacterial  
424 adhesion. Rsc Advances, 3(30), 12003-12020. <https://doi.org/10.1039/c3ra40497h>
- 425 Zheng, L., Qian, S. & Liu, X. Y. (2020). Induced antibacterial capability of TiO<sub>2</sub> coatings in visible  
426 light via nitrogen ion implantation. Transactions of Nonferrous Metals Society of China, 30(1),  
427 171-180. [https://doi.org/10.1016/S1003-6326\(19\)65189-7](https://doi.org/10.1016/S1003-6326(19)65189-7)
- 428 Zheng, Y. Y., Miao, J. J., Zhang, F. M., Cai, C., Koh, A., Simmons, T. J., Mousa, S. A. & Linhardt, R. J.  
429 (2016). Surface modification of a polyethylene film for anticoagulant and antimicrobial catheter.  
430 Reactive & Functional Polymers, 100, 142-150. 10.1016/j.reactfunctpolym.2016.01.013  
431